Desalination and Water Treatment
www.deswater.com

doi: 10.5004/dwt.2023.29597

295 (2023) 166–176
May

Enhanced removal of Cr(VI) of effectiveness and mechanism from wastewater using modified distiller grains-based biochar

Hengjun Tang[a], Biao Qiu[a], Jian Tang[a,b,c,d,*], Yi Liao[a], Guo Liu[b,c,*], Suyi Zhang[d], Zonghua Ao[d], Kai Shang[a]

[a]*School of Civil Engineering, Sichuan University of Science and Engineering, Zigong 643000, China, emails: tangtang100@126.com (J. Tang), 35128500@qq.com (H.J. Tang), qiubiao1998@163. com (B. Qiu), ly-001-1980@163.com (Y. Liao), sk727294941@163.com (K. Shang)*

[b]*State Key Laboratory of Geohazard Prevention and Geoenvironment Protection, Chengdu University of Technology, Chengdu 610059, China, email: liuguo@cdut.edu.cn (G. Liu)*

[c]*State Environmental Protection Key Laboratory of Synergetic Control and Joint Remediation for Soil and Water Pollution, Chengdu University of Technology, Chengdu 610059, China*

[d]*Luzhou Laojiao Company Limited, Luzhou 646000, China, emails: zhangsy1@lzlj.com (S.Y. Zhang), aozh1@lzlj.com (Z.H. Ao)*

Received 17 October 2022; Accepted 24 April 2023

ABSTRACT

This study aimed to explore the Cr(VI) removal performance and mechanism of distillers' grains-based biochar. Biochar was prepared at 600°C and modified with an alkaline solution (1 M KOH). In this study, factors affecting adsorption efficiencies such as biochar dosage (1~3 g/L), $pH_{initial}$ (2.0~7.0), Cr(VI) initial concentration (10~300 mg/L), and adsorption time (0–24 h) were explored. The results showed that compared with the original biochar, the adsorption efficiency of Cr(VI) on the modified biochar after treatment with KOH solution was increased by 3 times. Scanning electron microscopy and Fourier-transform infrared spectroscopy analysis indicated that the morphology and function of biochar changed significantly after modification. When the dosage of modified biochar reaches 3.0 g/L, the removal rate of Cr(VI) of 50 mg/L can reach 99.99%. The initial pH of the solution is an essential adsorption parameter to determine the adsorption capacity of biochar. The removal efficiency of Cr(VI) in the solution with lower pH is higher. The adsorption behavior of the modified biochar was more consistent with Freundlich isothermal adsorption model and the quasi-second-order kinetic equation. The theoretical equilibrium adsorption capacity Q_e of KBC-2, KBC-1, and BC were 29.54, 19.76, and 9.37 mg/g, respectively. Thermodynamic studies indicate that the adsorption of Cr(VI) by KABC-1, KABC-2, and BC is an automatic and endothermic process. In addition, the adsorption mechanism of Cr(VI) by modified distillers' grains biochar can be explained as the synergistic action of chemical and physical adsorption.

Keywords: Biochar; Distiller's grains; Modification; Heavy metal; Cr(VI)

1. Introduction

Chromium (Cr) is a mineral widely used in the electroplating industry. Its hexavalent state is highly toxic and carcinogenic to organisms. Chromate can irritate the skin and damage the respiratory system [1]. Therefore, restoring Cr(VI)-contaminated water bodies is significant. At present, the methods of remediation of Cr(VI) polluted water bodies include precipitation, electrolysis, ion exchange, and adsorption [2,3]. Among the treatment mentioned above methods, adsorption has become one of the most popular

* Corresponding authors.

adsorbents because of its wide range of raw materials for biochar preparation and environmental friendliness [4]. Many adsorbents have been developed and used, such as activated carbon [5,6], silica [7], biochar [8,9], and so on.

Biochar is a carbon-rich product produced by pyrolysis and carbonization of biomass under anoxic or anaerobic conditions. It has a large specific surface area, developed pore structure, and large oxygen-containing functional groups, showing good adsorption capacity. There are many kinds of raw materials for biochar preparation, primarily agricultural and forestry waste, livestock and poultry manure, and other biomass, such as wheat straw [10], rice husk [11], sawdust [12], cow dung [13], etc. Liquor grains are a by-product of sorghum, corn, and rice distillation of liquor. According to statistics, China's annual liquor production has exceeded 8.7 billion liters, a large country of liquor consumption and more than 35 million tons of distiller's grains are produced yearly [14]. Liquor grains, as solid waste produced in liquor production, are usually used as feed for pigs, cattle, poultry, and other animals, as well as a culture medium for edible fungi or a source of agricultural fertilizers. The amount of chemical development and utilization is limited [14,15]. To achieve greater resource utilization of distiller's grains and combined with the prominent phenomenon of environmental pollution, distiller's grains are prepared into biochar materials for research on environmental remediation.

However, although many studies have reported the application of biochar in the adsorption of heavy metal ions in water bodies, the adsorption of Cr(VI) using liquor distillers' grains biomass as raw material is still blank. In addition, the adsorption mechanism of Cr(VI) on this material is still to be discovered. Unfortunately, through the preliminary test, it is found that the adsorption capacity of this material on Cr(VI) is only 7.85 ± 0.52 mg/g. The general practice is modifying the biochar to improve distillers' grain adsorption capacity. The common ways are loaded metal oxide [16], ball milling modification [17], and acid and alkaline solution modification [18,19]. Potassium hydroxide (KOH) activation is a low-cost and efficient modification method, which can effectively improve the porosity, increase the specific surface area, and improve the adsorption performance [20]. Therefore, KOH will be used in the study to modify biochar.

This study prepared raw biochar and KOH-modified biochar from the distiller's grains and applied them to remove Cr(VI) in an aqueous solution. The primary purpose of this work is to (1) compare the adsorption capacity of raw distiller's grains biochar and KOH-modified biochar; (2) explore the effect of some external environmental factors (biochar dosage, pH, adsorption temperature, adsorption time, and initial concentration) on the effect of adsorption performance; (3) combined with X-ray photoelectron spectroscopy (XPS), Brunauer–Emmett–Teller (BET), Fourier-transform infrared spectroscopy (FTIR) and other characterization methods to explore the mechanism of Cr(VI) removal by modified distillers' grains biochar.

2. Materials and methods

2.1. Materials and instruments

The chemicals used in the study included diphenyl carbamide ($C_{13}H_{14}N_4O$, AR), hydrochloric acid (HCl, AR), potassium hydroxide (KOH, AR), potassium dichromate ($K_2Cr_2O_7$, AR), sulfuric acid (H_2SO_4, AR). The baijiu distiller's grains are collected from the solid waste produced by distilling in Luzhou Laojiao Co., Ltd., Sichuan Province, China. The baijiu vinasse is dried at 80°C, then crushed into 0.25 mm particles, stored as biomass raw materials, and used for composite materials.

2.2. Preparation of modified distillers, grains-based biochar

The 40.00 g stored vinasse distillers' grains biomass is put into a tube furnace, which is then filled with nitrogen to expel oxygen from the quartz tube (Zhengzhou Ansheng Scientific Instrument Co., Ltd., SK2-4-12TPB3, China), thus ensuring an anoxic environment inside the quartz tube during pyrolysis. The heating program of the tubular furnace is controlled as follows: the initial temperature is room temperature, the heating rate is 5°C/min, and the final temperature is 600°C. When the temperature increased to 600°C, the biochar obtained by holding at this temperature for 2 h was the original biochar (BC). Preparation of the modified biochar: the prepared BC and 1 M KOH were evenly mixed according to a mass ratio of 1:20 and stirred at room temperature for 3 h. After filtration, the surface was washed with ultra-pure water to be close to neutral to obtain KABC-1; KABC-2 was obtained by pyrolysis at 600°C for 1 h under the same heating procedure.

2.3. Characterization of modified distillers grains-based biochar

Scanning electron microscopy (SEM, Hitachi S-4800, Japan) was used to analyze the surface morphology of biochar samples before and after adsorption. At the same time, the specific surface area and pore volume of modified biochar were measured by a surface and pore size analyzer (Beside Instrument Technology Co., Ltd., 3H-2000PS2, China). X-ray photoelectron spectroscopy (XPS, Thermo Scientific™ ESCALAB™ 250Xi, USA) was performed to identify functional groups on the biochar surface and analyze the valence states of elements on the sample surface. The surface functional groups of biochar samples before and after adsorption were characterized by FTIR. FTIR (PerkinElmer Frontier, USA) was used to identify the characteristics of surface functional groups of modified vinasse distillers' grains-based biochar before and after adsorption, with wavenumbers ranging from 400 to 4,000 cm^{-1}.

2.4. Adsorption experiment

Cr(VI) stock solution (1,000 mg/L) was obtained by dissolving 2.829 g of $K_2Cr_2O_7$ powder in 1 L of ultra-pure water. The stock solution dilutes the Cr(VI) standard used in the experiment. All studies (dosing amount, kinetics, pH, and initial concentration on the effect of Cr(VI) removal) were conducted in 30 mL glass vials. In the study, Cr(VI) standard was taken to use 20 mL of solution in the sample vial, the pH of the solution was adjusted to 2.0 with 0.1 M HCl and NaOH, 2.5 g/L biochar was added, the adsorption temperature was 25°C, and after the vibration of the shaker at a constant temperature water bath at a speed of 250 rpm for 24 h, it was filtered through a 0.45 μm membrane to determine

the concentration of Cr(VI) of the filtered solution. In the study, the effects of biochar dosing amount (1.0–3.0 g/L), pH of the solution (2.0–7.0), adsorption time (0–1,440 min), and different initial concentrations (0–250 mg/L) on the adsorption performance of Cr(VI) were studied.

2.5. Data processing

This study used diphenylcarbazide spectrophotometry to measure the concentration of Cr(VI) in the filtered solution [21,22]. The removal efficiency and removal rate of Cr(VI) were calculated according to Eqs. (1) and (2), respectively.

$$q = \frac{(C_0 - C_e)}{M} V \quad (1)$$

$$\eta = \frac{(C_0 - C_e)}{C_0} \times 100\% \quad (2)$$

where C_0 and C_e are the initial and equilibration remanent Cr(VI) concentrations (mg/L), respectively; V is the initial Cr(VI) solution volume (L); M is the adsorbent dosage (g); η is the removal rate (%); q is the adsorption performance (mg/g).

3. Results and discussion

3.1. Yield analysis

The distillers' grains biomass (40.00 ± 0.01 g) was put into a tubular furnace (the initial temperature was room temperature at 5°C/min, and the pyrolysis temperature reached 600°C for 2 h). The weight of biochar was 14.46 ± 0.1 g, and the yield was 36.15%. After impregnation with KOH solution and pyrolysis, the product weighed 12.26 ± 0.1 g, yielding 30.65%. This yield compares favorably with other types of biochar.

3.2. Effect of different dosages on adsorption

Fig. 1 shows the adsorption quantity and removal rate of Cr(VI) when the adsorbent dosage is 1.0~3.0 g/L. Compared with BC, KBC-2, and KBC-1 have significantly improved adsorption capacity for Cr(VI) after modification. When the initial concentration of Cr(VI) in the solution was 50 mg/L, and the dosage of the three biochars (KBC-2, KBC-1, BC) was 1 g/L, the adsorption capacity of Cr(VI) was the largest, which were 29.84 ± 0.45, 17.73 ± 0.31, and 9.44 ± 0.43 mg/g, and the removal efficiencies were 59.68%, 35.46%, and 18.89%, respectively, which may be due to the lack of adsorption sites at low biochar dosage concentrations [23]. The study found that with the increase in biochar dosing, the adsorption volume of Cr(VI) decreased. When the amount of biochar dosing reached 3.0 g/L, the adsorption amount of KBC-2, KBC-1, and BC was reduced to 16.70 ± 0.11, 14.70 ± 0.22, and 7.84 ± 0.16 mg/g, respectively, but at this time, the removal rate of Cr(VI) in the solution of the three kinds of biochar was significantly increased relative to the dosing amount of 1 g/L. The removal rate reached 99.99%, 88.24%, and 47.06%, respectively, indicating that the amount of biochar dosing can provide more adsorption points, which is conducive to achieving all the adsorption of Cr(VI) in the aqueous solution. Considering that the removal rate of Cr(VI) can reach 99% when the dosage of modified biochar (KBC-2) is 2.5 g/L, the biochar concentration in subsequent experiments is 2.5 g/L.

3.3. Effect of initial pH of solution on adsorption

The pH of the solution is an essential factor in the adsorption performance. To study the effect of pH on the adsorption efficiency of modified biochar, the effect of the solution pH of 2.0–7.0 on the adsorption efficiency was investigated under the conditions of 2.5 g/L, the initial concentration of Cr(VI) was 100 mg/L, the adsorption temperature was 25°C, and the speed of 250 rpm oscillation was 24 h. The results are shown in Fig. 2.

It can be seen from Fig. 2 that the pH of the solution dramatically influences the adsorption efficiency. When the pH value of the solution is 2.0, the removal efficiency

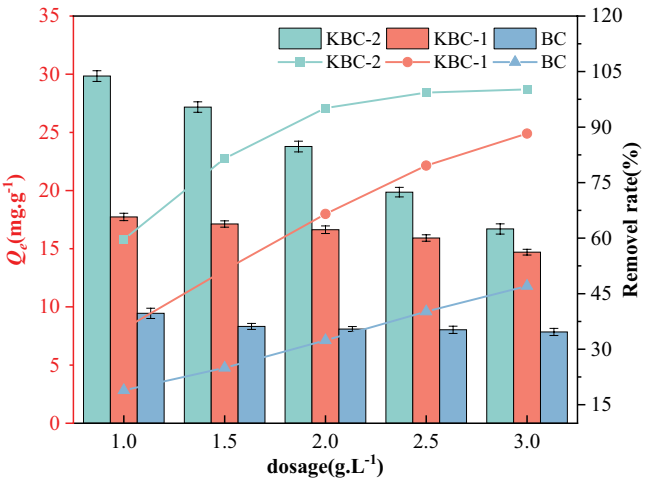

Fig. 1. Adsorption efficiency of biochar at different dosages.

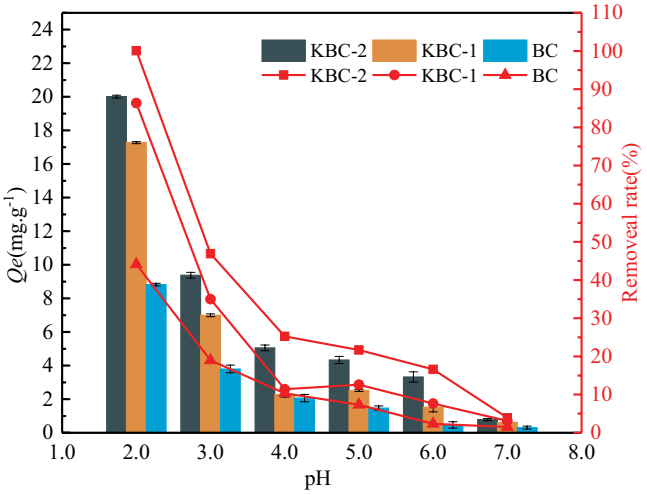

Fig. 2. Effect of pH on adsorption efficiency of biochar.

of alkaline modified biochar KBC-2 for Cr(VI) is better, the adsorption capacity reaches 20.01 ± 0.02 mg/g, and the removal rate reaches 99.98%. At this time, KBC-1 compared with the original biochar, the adsorption capacity of BC on Cr(VI) increased by 2.3 and 1.9 times, respectively, indicating that the adsorption performance was significantly improved after modification. With the increase in solution pH, KBC-2, KBC-1, and BC all showed a decreasing trend for the adsorption of Cr(VI), and the removal rate also kept the same decreasing trend as the adsorption, consistent with the conclusions of Liu et al. [24] and Rajapaksha et al. [25]. With the increase in pH value, the surface functional groups of biochar are deprotonated seriously, and the surface generates a net negative charge, which is negatively charged [26]. However, when the pH of the aqueous solution is 1.0~6.8, Cr(VI) is usually replaced by $HCrO_4^-$, $Cr_2O_7^{2-}$ form exists [24,27], which repels the negatively charged biochar on the surface, which is not conducive to the adsorption of Cr(VI). When the pH is 2.0 ± 0.1, the adsorption capacity of the three types of biochars is higher than that of the other pH. This may be due to the increased protonation of the biochar surface, which leads to more positive charges on the surface. Due to gravity, it is easier to interact with the negatively charged $HCrO_4^-$ and $Cr_2O_4^{2-}$ ions collide and combine, which is beneficial to adsorption [28].

3.4. Removal kinetics

In the study, the adsorption temperature was 25°C, the initial concentration of Cr(VI) was 100 mg/L, the pH of the solution was 2.0, and the amount of biochar dosing was 2.5 g/L, and the effect of adsorption time on the efficacy of modified biochar removal of Cr(VI) was explored, and the results are shown in Fig. 3.

It can be seen from Fig. 3 that the whole process from the time of adding the adsorbent to the adsorption reaches equilibrium can be divided into three stages: the fast adsorption stage, the slow adsorption stage, and the equilibrium stage. The 0~30 min stage belongs to the fast adsorption stage. In this stage, the adsorption capacity of KBC-2, KBC-1, and BC to Cr(VI) increases rapidly, reaching 18.61 ± 0.56, 12.68 ± 0.34, and 6.75 ± 0.36 mg/g, respectively. The reason for the rapid increase may be that in the initial stage of adsorption, the surface of biochar has a large amount of adsorption potential, so Cr(VI) is more likely to be adsorbed to the surface of biochar during the collision between Cr(VI) and biochar [29]. In the slow adsorption stage from 30 to 960 min, the adsorption capacity of KBC-2, KBC-1, and BC increased to 28.63 ± 0.58, 19.19 ± 0.44 and 9.44 ± 0.41 mg/g, respectively. The adsorption volume changed slightly from 960 to 1,440 min, and the adsorption reached equilibrium, and the adsorption amounts of the three kinds of biochar were 30.46 ± 0.56, 20.25 ± 0.47 and 9.49 ± 0.44 mg/L, respectively.

To study the adsorption process of Cr(VI) on the adsorption-modified biochar, nonlinear pseudo-first-order kinetics [Eq. (3)] and pseudo-second-order kinetics [Eq. (4)] were used to fit the adsorption test data. The fitting parameters are shown in Table 1.

$$\log\left(Q_e - Q_t\right) = \log Q_e - \frac{k_1}{2.303}t \tag{3}$$

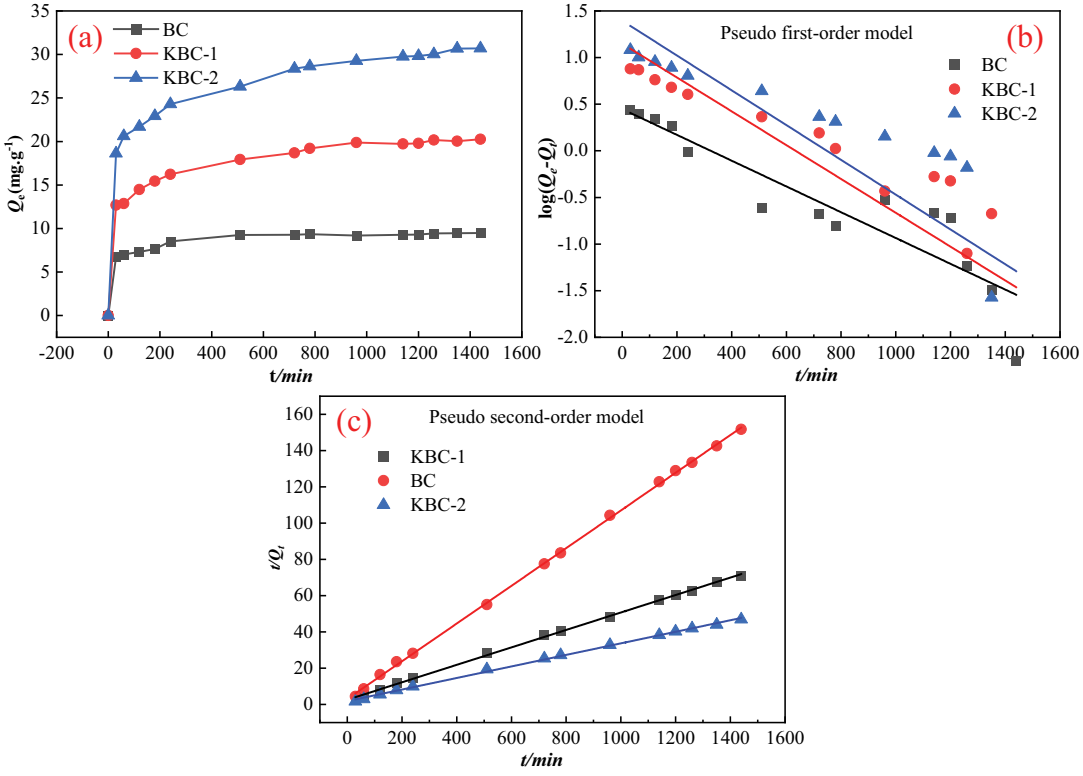

Fig. 3. Effect of time on adsorption efficiency of biochar.

Table 1
Kinetic fitting parameters

Adsorbent	Pseudo-first-order model			Pseudo-second-order model		
	Q_e (mg/g)	k_1 (min^{-1})	R^2	Q_e (mg/g)	k_2 (g/mg·min)	R^2
KBC-2	24.86	0.00318	0.58769	31.4	0.00055	0.99811
KBC-1	14.10	0.00417	0.61942	20.78	0.0009	0.99876
BC	2.80	0.00319	0.82584	9.62	0.00358	0.99954

$$\frac{t}{Q_t} = \frac{1}{Q_e} + \frac{1}{k_2 Q_e^2} \tag{4}$$

where Q_t and Q_e are specific time and equilibration Cr(VI) concentrations (mg/g), respectively. k_1 (min^{-1}) and k_2 (g(mg·min)) are the rate constants of the pseudo-first-order model and pseudo-second-order model kinetic equations, respectively.

The pseudo-first-order and pseudo-second-order model fitting parameters of Cr(VI) adsorption on BC, KABC-1, and KABC-2 are shown in Table 1. The quasi-first-order kinetic model suggests that the limiting factor of adsorption is the resistance of mass transfer within particles. The pseudo-second-order kinetic model suggests that the main limiting factor of adsorption is the adsorption mechanism. By comparing the fitting parameters of pseudo-first-order and pseudo-second-order models, it can be seen from Table 1 that the pseudo-second-order kinetic model has a higher fitting degree, and the equilibrium adsorption capacity Q_e (31.40, 20.78, and 9.62 mg/g) calculated and fitted by the pseudo-second-order model is closer to the actual adsorption capacity (30.46 ± 0.32, 20.25 ± 0.53, and 9.49 ± 0.38 mg/g). These results indicate that several factors, including external liquid film diffusion, surface adsorption, and intraparticle diffusion, influence the adsorption of Cr(VI) by distillers' grains biochar. The adsorption process based on pseudo-second-order kinetics assumes that the adsorption rate is controlled by chemical reaction [2], and the adsorption of Cr(VI) by distillers' grains biochar is concluded as chemical adsorption. The results of FTIR and XPS characterization prove this conclusion.

3.5. Adsorption isotherms

The effects of the initial concentration of Cr(VI) (0–300 mg/g) on the removal efficiency of modified biochar were investigated at adsorption temperatures of 25°C, 45°C, and 65°C, solution pH 2.0, and biochar dosage of 2.5 g/L, respectively—the Langmuir isothermal model [Eq. (5)] and Freundlich model [Eq. (6)] were used to nonlinear fit the data [30,31]. The results are shown in Fig. 4 and Table 2.

$$Q_e = \frac{Q_m K_L C_e}{1 + K_F C_e} \tag{5}$$

$$Q_e = K_F C_e^{1/n} \tag{6}$$

where Q_e and C_e are the adsorption quantity (mg/g) and remanent concentrations (mg/L) of Cr(VI) at the moment of adsorption equilibrium, respectively; K_L (L/mg) is Langmuir adsorption constant, K_F (L/mg) is Freundlich adsorption constant; n is Freundlich constant of the reaction adsorption strength.

The adsorption capacity of KBC-1, KBC-2, and BC also increased with the increase in initial Cr(VI) in the solution, which may be because the doubling of the initial concentration leads to more contact opportunities between the adsorbent and Cr(VI). The adsorption capacity increased [32]. It can be seen from Table 2 that the Freundlich isotherm adsorption model is more suitable for the adsorption process of Cr(VI) by KBC-1, KBC-2, and BC, reflecting that the adsorption process is non-uniform adsorption. The $1/n$ values that characterize the adsorption strength in the fitted data are between 0.1 and 0.5, indicating that KBC-1, KBC-2, and BC have strong adsorption capacity for Cr(VI).

In addition, it was found that with the increase in temperature, the adsorption capacity of KBC-1, KBC-2, and BC to Cr(VI) increased, indicating that the temperature increase can effectively increase the adsorption capacity, and the adsorption process is an endothermic reaction. Thermodynamic studies were calculated using [Eqs. (7)~(9)].

$$\Delta G^\circ = -RT \ln K_F \tag{7}$$

$$\Delta G^\circ = \Delta H^\circ - T\Delta S^\circ \tag{8}$$

$$\ln K_F = \frac{\Delta H^\circ}{RT} + \frac{\Delta S^\circ}{R} \tag{9}$$

where K_F is the Freundlich adsorption constant, L/mg; ΔG° is the Gibbs free energy of adsorption, kJ/mol; ΔH° is the enthalpy change, kJ/mol; R is the ideal gas constant, 8.314×10^{-3} kJ/(mol·K); ΔS° is the adsorption entropy change, J/(mol·K); T is the adsorption temperature, K.

The thermodynamic parameters ΔG°, ΔH°, ΔS° of the adsorption of Cr(VI) by KBC-2, KBC-1, and BC are shown in Table 3. At 298, 318, and 338 K, the Gibbs free energies of the three biochars were negative ($\Delta G^\circ < 0$), indicating that the adsorption of Cr(VI) by the three biochar was spontaneous. At the same time, ΔH° is positive, indicating that the adsorption reaction is an endothermic process [33], and increasing the temperature can improve the adsorption efficiency.

3.6. Modified biochar characterization

The previous experiments indicate that the adsorption efficiency of Cr(VI) in an aqueous solution is greatly improved after BC is impregnated and modified in a KOH

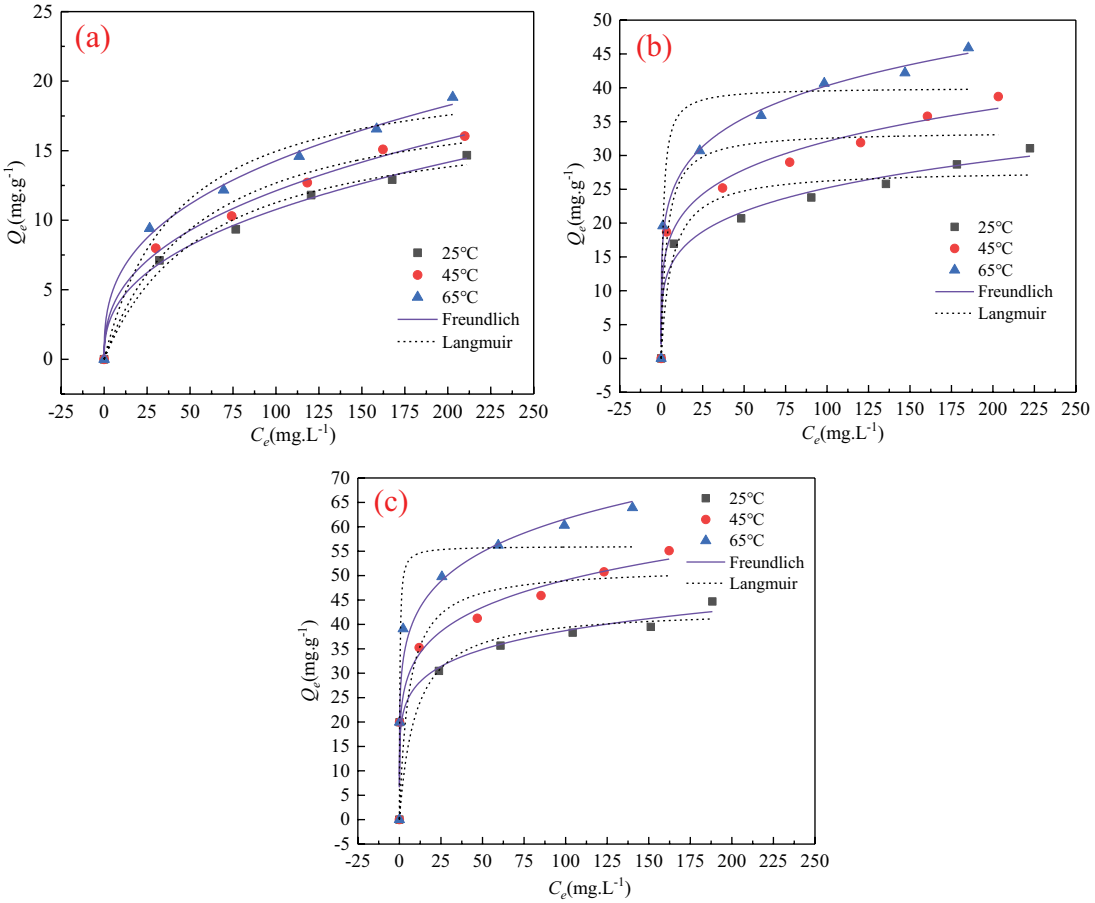

Fig. 4. Effect of concentration on adsorption efficiency of biochar.

Table 2
Data fitting of isothermal adsorption model

Adsorbent	T (°C)	Langmuir			Freundlich		
		Q_m (mg/g)	K_L (L/mg)	R^2	1/n	K_F (mg$^{(-1-1/n)}$/L$^{1/n}$·g)	R^2
KBC-2	25	43.28	0.10113	0.660	0.15	19.2858	0.920
	45	51.71	0.17594	0.776	0.17	22.0275	0.956
	65	56.01	1.24035	0.908	0.16	28.5075	0.954
KBC-1	25	27.87	0.15928	0.920	0.21	9.41775	0.973
	45	33.57	0.31487	0.898	0.20	12.7330	0.977
	65	40.02	0.83865	0.913	0.18	17.4097	0.986
BC	25	17.89	0.01698	0.983	0.39	1.74592	0.996
	45	19.67	0.01812	0.978	0.38	2.04051	0.995
	65	21.25	0.02371	0.972	0.35	2.79155	0.995

solution. To explore the removal mechanism of Cr(VI) in an aqueous solution by modified biochar, a series of methods are used to analyze KABC-2 before and after the reaction with Cr(VI).

As shown in Fig. 5, SEM images depict the porous properties of distillers' grains-based biochar before and after modification and after reaction with Cr(VI). The original biochar (BC) surface is uneven and blocky, without an obvious porous structure, and the pore structure is poorly developed. At the same magnification, it was found that the surface of the modified KABC-2 showed a honeycomb-like pore structure and a more developed pore structure. At the same time, small pieces of carbon material are attached to the pores, resulting in the material's non-smooth morphology, which is caused by alkaline solution erosion on the BC surface [34]. The BET surface area, pore

size, and total pore volume of BC were 98.19 m^2/g, 3.75 nm, and 0.0922 cm^3/g, respectively, the BET surface area and total pore volume of KBC-2 were increased to 239.65 m^2/g and 0.2115 cm^3/g, respectively, the pore size is reduced to 3.53 nm, which belongs to the mesoporous material. The increase in total pore volume and specific surface area can provide more adsorption sites, which will facilitate the adsorption of KBC-2 to Cr(VI). However, after the reaction with Cr(VI), the surface is rougher and presents the collapse of part of the pore wall, which the corrosion of biochar may cause in the acidic solution and the adsorption of the Cr(VI) coating [24].

Fig. 6 shows the FTIR spectra of surface functional groups before and after Cr(VI) adsorption by KBC-2. KBC-2 contains a variety of functions, such as C–H, C=O, C–O, and –OH. These groups may be responsible for the binding of Cr(VI) and the proton and electron reduction of Cr(VI) to Cr(III). The characteristic peak near 3,450 cm^{-1} is the stretching vibration of the alcohol/phenol hydroxyl group (–OH) [35,36]. The peak near 2,926 and 2,855 cm^{-1} is the aliphatic compound C–H's asymmetric tensile vibration peak [24,37].

Table 3
Thermodynamic parameters

Adsorbent	T (K)	$\Delta G°$ (kJ/mol)	$\Delta H°$ (kJ/mol)	$\Delta S°$ (J(mol·K))
KBC-2	298	–7.33	8.12	51.65
1	318	–8.17	1	1
1	338	–9.41	1	1
KBC-1	298	–5.55	12.85	61.69
1	318	–6.72	1	1
1	338	–8.03	1	1
BC	298	–1.38	9.75	37.10
1	318	–1.88	1	1
1	338	–2.88	1	1

The peaks at 1,632 and 1,565 cm^{-1} are thought to be associated with aromatic ring C=C or carboxyl C=O bonds [24]. Si–O–Si symmetric and O–Si–O bending vibrations were observed at 797 and 466 cm^{-1} absorption peaks [38]. The characteristic peak at 1,084 cm^{-1} is C=O in the ether [1]. After adsorption, Cr(VI) interacts with functional groups on the surface of biochar, resulting in significant changes in FTIR spectra. After Cr(VI) adsorption, C=O shifted at 1,084 cm^{-1}, and the peak intensity increased, indicating that some functional groups were oxidized to C=O. The position of the characteristic peak of the hydroxyl functional group moved from 3,450 to 3,418 cm^{-1}, the intensity of the peak was weakened, and the number of oxygen-containing groups decreased, indicating that –OH may have participated in the reaction during the adsorption process.

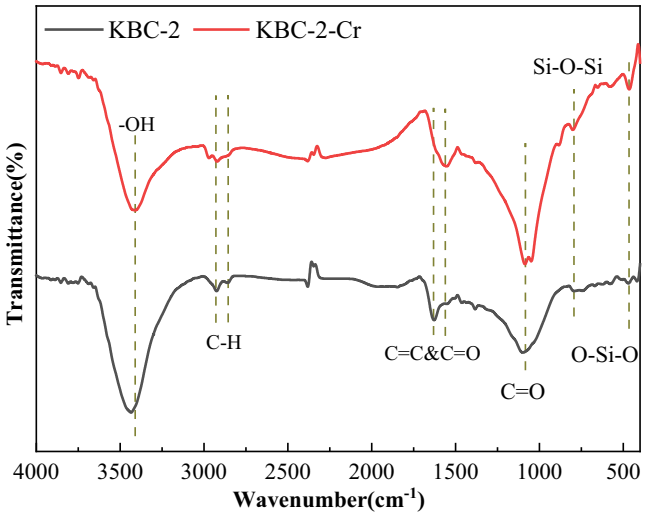

Fig. 6. Fourier-transform infrared spectra of KBC-2 before and after adsorption.

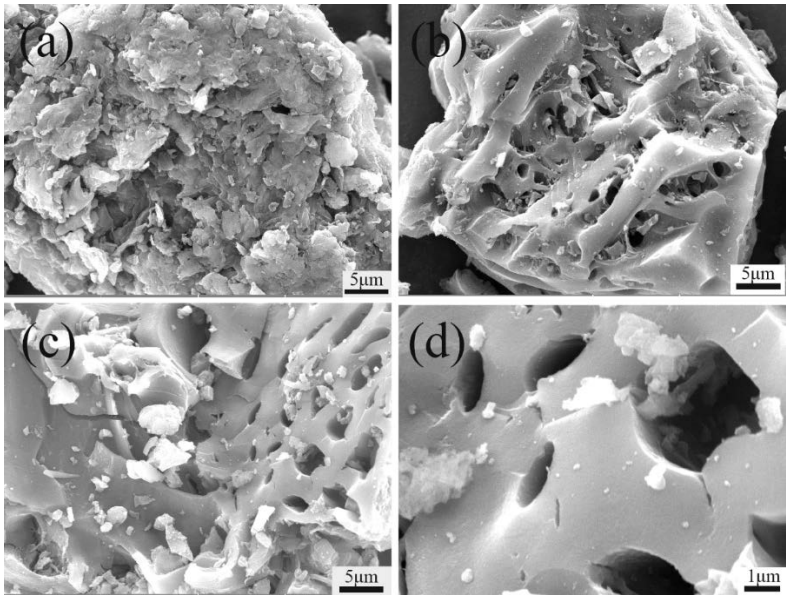

Fig. 5. Scanning electron microscopy images of (a,b) BC and KBC before adsorption, respectively and (c,d) KBC after adsorption.

To elaborate on the mechanism of KBC-2 adsorption of Cr(VI) in an aqueous solution, XPS technology was used to analyze the chemical states of the main elements of biochar.

The XPS technique was used to analyze the chemical composition of KBC-2 before and after adsorption. It can be seen from Fig. 7c and d that the XPS spectra of C 1s before and after the reaction of KBC-2 are similar, and they are all divided into three peaks by fitting, representing three different functional groups. The peaks at 284.8, 285.4, and 288.1 eV binding energies are attributed to C–C, C–O, and C=O (carbonyl) groups, respectively [24]. By calculating the ratio of the single peak area to the total peak area of all functional groups, it was found that the content of functional groups of C 1s also changed significantly after the reaction with Cr(VI). The proportion of the C–C functional group increased from 52.81% to 56.12%. The content of the C–O functional group decreased from 31.66% before the reaction to 31.21%. The proportion of the C=O group decreased from 15.53% to 12.67%. Fig. 7e and f show the XPS atlas of O 1s before and after the reaction of KBC-2. The peak at 532.6 eV was attributed to O–C=O in the carboxyl group [39], O–H [40] at 530.84 eV, C–O at 533.8 eV, and C=O at 531.5 eV, which is consistent with the XPS C 1s spectrum. After the reaction, the content of oxygen-containing functional groups on the surface of KBC-2 also changed. After adsorption, the content of O–C=O in the carboxyl group decreased from 43.14% to 32.97%. The content of C–O decreased from 20.14% to 13.48%. The contents of C=O and O–H increased from 30.65% and 6.16% to 35.17% and 18.37%, respectively. The contents of C–O and O–C=O decrease, but the contents of the C=O group increase, which may be because the C–O and O–C=O groups are oxidized to C=O in reacting with Cr(VI) under acidic conditions [41,42]. The presence of Cr 2p in XPS Fig. 7a indicates that Cr has been successfully adsorbed on the surface of biochar. The high-resolution XPS energy level spectrum after adsorption of KBC-2 (Fig. 7b) consists of two wide peaks, one of which is Cr 2p1/2 and the other is Cr 2p3/2. The binding

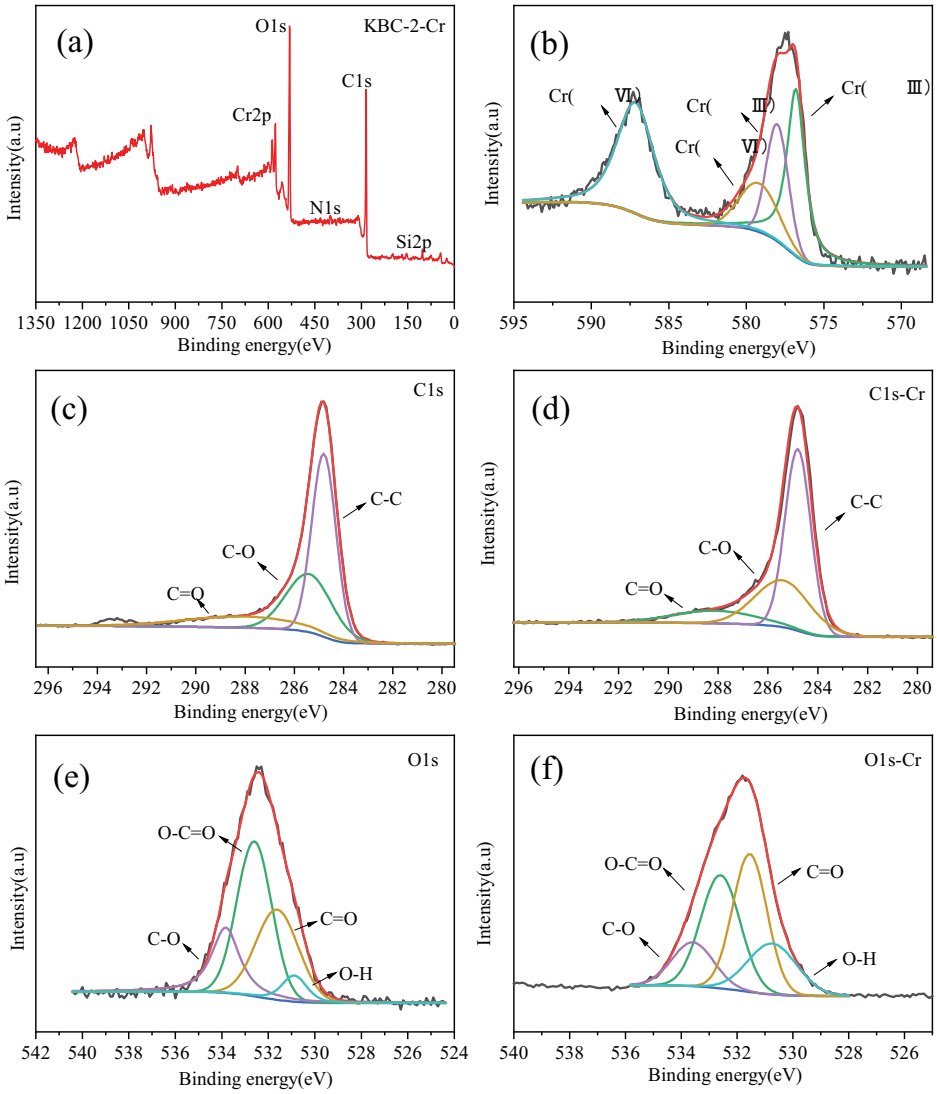

Fig. 7. X-ray photoelectron spectroscopy spectra of KBC-2 full range after reaction (a), Cr 2p (b) after reaction, C 1s ((c) before and (d) after reaction), O 1s (e) before and (f) after the reaction.

energies of the two peaks are 587.24 and 577.41 eV, respectively. Cr 2p3/2 deconvolution peaks can be divided into 579.2, 577.9, and 576.9 eV binding energy peaks, among which the first peak is the characteristic peak of Cr(VI), representing $HCrO_4^-$. The last two peaks are Cr(III), attributed to $Cr(OH)_3$ and Cr_2O_3 [24], respectively. According to the analysis of Cr 2p spectra, it is found that Cr compounds such as Cr_2O_3 and $Cr(OH)_3$ exist. Fig. 7b shows that after Cr(VI) is adsorbed on KBC-2, a part of Cr(VI) will be reduced to Cr(III) with low toxicity. They indicate precipitation, reduction, and complexation in the adsorption mechanism of Cr(VI) by KBC-2.

3.7. Removal mechanism

Based on biochar adsorption experiments in different pH solutions, it can be seen that the adsorption mechanism of Cr(VI) removal by KBC-2 includes electrostatic interaction. The functional groups on the surface of KBC-2 are protonated with H^+ in the solution to form positively charged $–OH^{2+}$ and $–COOH^{2+}$. Under electrostatic attraction, KBC-2, with the net positive charge on the surface, attracts and collides with anions such as $HCrO_4^-$ and $Cr_2O_7^{2-}$ in the solution and attaches to the adsorption sites on the biochar surface.

Biochar surface contains many oxygen-containing functional groups, which can be used as electron donors to reduce Cr(VI) to Cr(III). From the XPS Cr 2p spectra of KBC-2, Cr(III) appears after adsorption, indicating that reduction reactions accompany the adsorption process. Combined with FTIR analysis, the positions of –OH, C=O, and C–O characteristic peaks before and after the adsorption of KBC-2 were found to shift to a certain extent after the adsorption, which was caused by the complexation of oxygen-containing functional groups with Cr(VI) and the formation of Cr precipitate [43,44]. The equation involved is as follows:

$$HCrO_4^- + 7H^+ + 3e^- \rightarrow Cr^{3+} + H_2O \quad (10)$$

$$Cr_2O_7^- + 14H^+ + 6e^- \rightarrow 2Cr^{3+} + 7H_2O \quad (11)$$

$$Cr^{3+} + 3OH^- \rightarrow Cr(OH)_3 \downarrow \quad (12)$$

Based on the above analysis, the adsorption process of Cr(VI) in aqueous solution by KBC-2 can be described as follows (Fig. 8): Cr(VI) and the protonated KBC-2 collide with each other and bind to the adsorption site under the action of static electricity. Part of Cr(VI) is reduced to Cr(III) in the acidic environment, and complexation occurs with Cr(VI) under the participation of –OH, C=O, C–O, etc., and more stably adsorbs on the surface of KBC-2 through the action of chemical bonds.

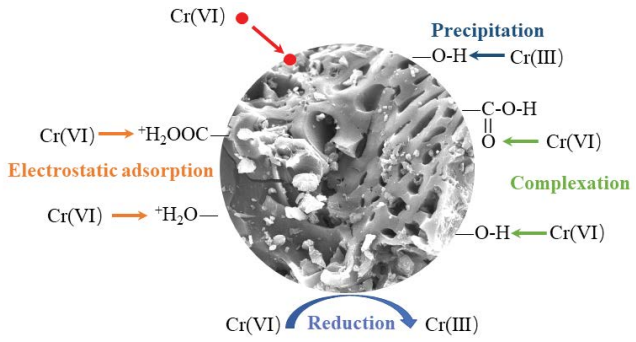

Fig. 8. Mechanism of Cr(VI) removal by KBC-2.

4. Conclusions

The modified distillers' grains-based biochar (KBC-2) is more effective in removing Cr(VI) from the solution than the original biochar (BC). After KOH modification, the surface area of distillers' grains biochar increased from 98.18 to 239.65 m^2/g, and the total pore volume increased from 0.0922 to 0.2115 cm^3/g. Such changes will be more favorable for Cr(VI) adsorption. The results prove that the initial pH of the solution significantly influences the adsorption property of KBC-2, and the adsorption property is the best under the condition of pH 2.0 ± 0.1. The adsorption equilibrium of Cr(VI) was reached about 16 h after the adsorption reaction of KABC-2. In addition, the adsorption of Cr(VI) by KABC-2 in water is a spontaneous and endothermic process. The adsorption mechanism of Cr(VI) on KABC-2 includes electrostatic attraction, reduction, and recombination reactions. The Freundlich isothermal model and pseudo-second-order kinetic model better fit the adsorption process of Cr(VI) in water with KBC-2.

Acknowledgments

This research was financially supported by the Opening fund of State Key Laboratory of Geohazard Prevention and Geoenvironment Protection (No. SKLGP2023K016), Open Project of State Environmental Protection Key Laboratory of Synergetic Control and Joint Remediation for Soil and Water Pollution (No. GHBK-2022-003), Sichuan Science and Technology Program (No. 2021YJ0342), the Key Research and Development Project of Luzhou Science and Technology Planning Programs (No. 2020-SYF-20), Talent Introduction Funds of the Sichuan University of Science and Engineering (No. 2020RC23), Luzhou Laojiao Limited Company Fund (No. 2022NB11), National College Student's innovation and entrepreneurship training program (No. 202110622016), and the Innovation Fund of Postgraduate, Sichuan University of Science & Engineering (D10501705).

References

[1] A.A. Khan, S.R. Naqvi, I. Ali, M. Arshad, H. AlMohamadi, U. Sikandar, Algal-derived biochar as an efficient adsorbent for removal of Cr(VI) in textile industry wastewater: non-linear isotherm, kinetics and ANN studies, Chemosphere, 316 (2023) 137826, doi: 10.1016/j.chemosphere.2023.137826.
[2] A. Shakya, M. Vithanage, T. Agarwal, Influence of pyrolysis temperature on biochar properties and Cr(VI) adsorption from water with groundnut shell biochars: mechanistic approach, Environ. Res., 215 (2022) 114243, doi: 10.1016/j.envres.2022.114243.
[3] A.Y. Li, W.Z. Ge, L.H. Liu, G.H. Qiu, Preparation, adsorption performance and mechanism of MgO-loaded biochar in wastewater treatment: a review, Environ. Res., 212 (2022) 113341, doi: 10.1016/j.envres.2022.113341.

[4] H.B. Li, X.L. Dong, E.B. da Silva, L.M. de Oliveira, Y.S. Chen, L.Q. Ma, Mechanisms of metal sorption by biochars: Biochar characteristics and modifications, Chemosphere, 178 (2017) 466–478.
[5] X. Wang, X. Liu, H. Wen, K. Guo, H. Brendon, D. Liu, A green, efficient reductive N-formylation of nitro compounds catalyzed by metal-free graphitic carbon nitride supported on activated carbon, Appl. Catal., B, 321 (2022) 122042, doi: 10.1016/j.apcatb.2022.122042.
[6] F.C. Su, F. Wang, C.S. Zhang, T.L. Lu, S. Zhang, R.Q. Zhang, X. Qi, P.P. Liu, Ameliorating substance accessibility for microorganisms to amplify toluene degradation and power generation of microbial fuel cell by using activated carbon anode, J. Cleaner Prod., 377 (2022) 134481, doi: 10.1016/j.jclepro.2022.134481.
[7] A. Yamaguchi, A. Ishii, T. Kamijo, Influence of ionic strength and temperature on adsorption of tetrakis-*N*-methylpyridyl porphyrin onto mesoporous silica, Colloids Surf., A, 655 (2022) 130262, doi: 10.1016/j.colsurfa.2022.130262.
[8] R. Isaac, S. Siddiqui, Sequestration of Ni(II) and Cu(II) using $FeSO_4$ modified *Zea mays* husk magnetic biochar: isotherm, kinetics, thermodynamic studies and RSM, J. Hazard. Mater. Adv., 8 (2022) 100162, doi: 10.1016/j.hazadv.2022.100162.
[9] L.C. Duan, Q.H. Wang, J.N. Li, F.H. Wang, H. Yang, B.L. Guo, Y. Hashimoto, Zero valent iron or Fe_3O_4-loaded biochar for remediation of Pb contaminated sandy soil: sequential extraction, magnetic separation, XAFS and ryegrass growth, Environ. Pollut., 308 (2022) 119702, doi: 10.1016/j.envpol.2022.119702.
[10] Y.Y. Cao, G.H. Shen, Y. Zhang, C.F. Gao, Y.F. Li, P.Z. Zhang, W.H. Xiao, L.J. Han, Impacts of carbonization temperature on the Pb(II) adsorption by wheat straw-derived biochar and related mechanism, Sci. Total Environ., 692 (2019) 479–489.
[11] T.H. Pham, T.T.H. Chu, D.K. Nguyen, T.K.O. Le, S.A. Obaid, S.A. Alharbi, J. Kim, M.V. Nguyen, Alginate-modified biochar derived from rice husk waste for improvement uptake performance of lead in wastewater, Chemosphere, 307 (2022) 135956, doi: 10.1016/j.chemosphere.2022.135956.
[12] F. Liu, R.X. Fang, X.F. Wang, J. Liu, Y. Li, The reaction characteristics and mechanism of pine sawdust chemical-looping gasification based on $CoFe_2O_4$ oxygen carrier, Renewable Energy, 195 (2022) 1300–1309.
[13] S. Hou, S.Y. Jia, J.J. Jia, Z.G. He, G.R. Li, Q.T. Zuo, H.F. Zhuang, Fe_3O_4 nanoparticles loading on cow dung based activated carbon as an efficient catalyst for catalytic microbubble ozonation of biologically pretreated coal gasification wastewater, J. Environ. Manage., 267 (2020) 110615, doi: 10.1016/j.jenvman.2020.110615.
[14] L. Peng, X.Y. Kong, Z.M. Wang, A. Ai-lati, Z.W. Ji, J. Mao, Baijiu vinasse as a new source of bioactive peptides with antioxidant and anti-inflammatory activity, Food Chem., 339 (2021) 128159, doi: 10.1016/j.foodchem.2020.128159.
[15] Y.Z. Wang, H.L. Liu, D.W. Zhang, J.M. Liu, J. Wang, S. Wang, B.G. Sun, Baijiu vinasse extract scavenges glyoxal and inhibits the formation of N^{ε}–carboxymethyllysine in dairy food, Molecules, 24 (2019) 1526, doi: 10.3390/molecules24081526.
[16] Y.J. Chen, R. Ma, X.C. Pu, X.Y. Fu, X.Y. Ju, M. Arif, X.Q. Yan, J. Qian, Y. Liu, The characterization of a novel magnetic biochar derived from sulfate-reducing sludge and its application for aqueous Cr(VI) removal through synergistic effects of adsorption and chemical reduction, Chemosphere, 308 (2022) 136258, doi: 10.1016/j.chemosphere.2022.136258.
[17] L. Zhao, Y. Zhang, L. Wang, H.H. Lyu, S.Y. Xia, J.C. Tang, Effective removal of Hg(II) and MeHg from aqueous environment by ball milling aided thiol-modification of biochars: effect of different pyrolysis temperatures, Chemosphere, 294 (2022) 133820, doi: 10.1016/j.chemosphere.2022.133820.
[18] Y.T. Han, J.J. Zheng, C. Jiang, F. Zhang, L.C. Wei, L. Zhu, Hydrochloric acid-modified algal biochar for the removal of *Microcystis aeruginosa*: coagulation performance and mechanism, J. Environ. Chem. Eng., 10 (2022) 108903, doi: 10.1016/j.jece.2022.108903.
[19] V.-T. Nguyen, T.-B. Nguyen, C.P. Huang, C.-W. Chen, X.-T. Bui, C.-D. Dong, Alkaline modified biochar derived from spent coffee ground for removal of tetracycline from aqueous solutions, J. Water Process Eng., 40 (2021) 101908, doi: 10.1016/j.jwpe.2020.101908.
[20] F. Lü, X.M. Lu, S.S. Li, H. Zhang, L.M. Shao, P.J. He, Dozens-fold improvement of biochar redox properties by KOH activation, Chem. Eng. J., 429 (2022) 132203, doi: 10.1016/j.cej.2021.132203.
[21] Y. Qiu, Q. Zhang, B. Gao, M. Li, Z. Fan, W.J. Sang, H.R. Hao, X.N. Wei, Removal mechanisms of Cr(VI) and Cr(III) by biochar supported nanosized zero-valent iron: synergy of adsorption, reduction and transformation, Environ. Pollut., 265 (2020) 115018, doi: 10.1016/j.envpol.2020.115018.
[22] C.E. Turick, W.A. Apel, A bioprocessing strategy that allows for the selection of Cr(VI)-reducing bacteria from soils, J. Ind. Microbiol. Biotechnol., 18 (1997) 247–250.
[23] X.D. Wang, J. Xu, J. Liu, J. Liu, F. Xia, C.C. Wang, R.A. Dahlgren, W. Liu, Mechanism of Cr(VI) removal by magnetic greigite/biochar composites, Sci. Total Environ., 700 (2020) 134414, doi: 10.1016/j.scitotenv.2019.134414.
[24] N. Liu, Y.T. Zhang, C. Xu, P. Liu, J. Lv, Y.Y. Liu, Q.Y. Wang, Removal mechanisms of aqueous Cr(VI) using apple wood biochar: a spectroscopic study, J. Hazard. Mater., 384 (2020) 121371, doi: 10.1016/j.jhazmat.2019.121371.
[25] A.U. Rajapaksha, Md. S. Alam, N. Chen, D.S. Alessi, A.D. Igalavithana, D.C.W. Tsang, Y.S. Ok, Removal of hexavalent chromium in aqueous solutions using biochar: chemical and spectroscopic investigations, Sci. Total Environ., 625 (2018) 1567–1573.
[26] J.-j. Pan, J. Jiang, R.-k. Xu, Removal of Cr(VI) from aqueous solutions by Na_2SO_3/$FeSO_4$ combined with peanut straw biochar, Chemosphere, 101 (2014) 71–76.
[27] X.X. Huang, Y.G. Liu, S.B. Liu, X.F. Tan, Y. Ding, G.M. Zeng, Y.Y. Zhou, M.M. Zhang, S.F. Wang, B.H. Zheng, Effective removal of Cr(VI) using β-cyclodextrin–chitosan modified biochars with adsorption/reduction bifuctional roles, RSC Adv., 6 (2016) 94–104.
[28] X.F. Tan, Y.G. Liu, G.M. Zeng, X. Wang, X.J. Hu, Y.L. Gu, Z.Z. Yang, Application of biochar for the removal of pollutants from aqueous solutions, Chemosphere, 125 (2015) 70–85.
[29] F.-X. Dong, L. Yan, X.-H. Zhou, S.-T. Huang, J.-Y. Liang, W.-X. Zhang, Z.-W. Guo, P.-R. Guo, W. Qian, L.-J. Kong, W. Chu, Z.-H. Diao, Simultaneous adsorption of Cr(VI) and phenol by biochar-based iron oxide composites in water: performance, kinetics and mechanism, J. Hazard. Mater., 416 (2021) 125930, doi: 10.1016/j.jhazmat.2021.125930.
[30] Z. Qiu, J.W. Tang, J.H. Chen, Q.H. Zhang, Remediation of cadmium-contaminated soil with biochar simultaneously improves biochar's recalcitrance, Environ. Pollut., 256 (2020) 113436, doi: 10.1016/j.envpol.2019.113436.
[31] M.P. Tong, L. He, H.F. Rong, M. Li, H.J. Kim, Transport behaviors of plastic particles in saturated quartz sand without and with biochar/Fe_3O_4-biochar amendment, Water Res., 169 (2020) 115284, doi: 10.1016/j.watres.2019.115284.
[32] M.A. Badawi, N.A. Negm, M.T.H. Abou Kana, H.H. Hefni, M.M. Abdel Moneem, Adsorption of aluminum and lead from wastewater by chitosan-tannic acid modified biopolymers: isotherms, kinetics, thermodynamics and process mechanism, Int. J. Biol. Macromol., 99 (2017) 465–476.
[33] Y.N. He, J.B. Chen, J.P. Lv, Y.M. Huang, S.X. Zhou, W.Y. Li, Y.T. Li, F.Q. Chang, H.C. Zhang, T. Wågberg, G.Z. Hu, Separable amino-functionalized biochar/alginate beads for efficient removal of Cr(VI) from original electroplating wastewater at room temperature, J. Cleaner Prod., 373 (2022) 133790, doi: 10.1016/j.jclepro.2022.133790.
[34] L.W. Wang, N.S. Bolan, D.C.W. Tsang, D. Hou, Green immobilization of toxic metals using alkaline enhanced rice husk biochar: effects of pyrolysis temperature and KOH concentration, Sci. Total Environ., 720 (2020) 137584, doi: 10.1016/j.scitotenv.2020.137584.
[35] Y.F. Ma, Y. Qi, L. Yang, L. Wu, P. Li, F. Gao, X.B. Qi, Z.L. Zhang, Adsorptive removal of imidacloprid by potassium hydroxide activated magnetic sugarcane bagasse biochar: adsorption efficiency, mechanism and regeneration, J. Cleaner Prod., 292 (2021) 126005, doi: 10.1016/j.jclepro.2021.126005.

[36] G.C. Yin, X.W. Song, L. Tao, B. Sarkar, A.K. Sarmah, W.X. Zhang, Q.T. Lin, R.B. Xiao, Q.J. Liu, H.L. Wang, Novel Fe-Mn binary oxide-biochar as an adsorbent for removing Cd(II) from aqueous solutions, Chem. Eng. J., 389 (2020) 124465, doi: 10.1016/j.cej.2020.124465.
[37] S.S. Bai, L. Wang, F. Ma, S.S. Zhu, T. Xiao, T.M. Yu, Y.J. Wang, Self-assembly biochar colloids mycelial pellet for heavy metal removal from aqueous solution, Chemosphere, 242 (2020) 125182, doi: 10.1016/j.chemosphere.2019.125182.
[38] S.Q. Shi, J.K. Yang, S. Liang, M.Y. Li, Q. Gan, K. Xiao, J.P. Hu, Enhanced Cr(VI) removal from acidic solutions using biochar modified by Fe_3O_4@SiO_2-NH_2 particles, Sci. Total Environ., 628–629 (2018) 499–508.
[39] M. Genovese, J.H. Jiang, K. Lian, N. Holm, High capacitive performance of exfoliated biochar nanosheets from biomass waste corn cob, J. Mater. Chem. A, 3 (2015) 2903–2913.
[40] L.X. Zhang, S.Y. Tang, F.X. He, Y. Liu, W. Mao, Y.T. Guan, Highly efficient and selective capture of heavy metals by poly(acrylic acid) grafted chitosan and biochar composite for wastewater treatment, Chem. Eng. J., 378 (2019) 122215, doi: 10.1016/j.cej.2019.122215.
[41] W.F. Liu, J. Zhang, C.L. Zhang, L. Ren, Preparation and evaluation of activated carbon-based iron-containing adsorbents for enhanced Cr(VI) removal: mechanism study, Chem. Eng. J., 189 (2012) 295–302.
[42] N. Liu, Y.T. Zhang, C. Xu, P. Liu, J. Lv, Y.Y. Liu, Q.Y. Wang, Removal mechanisms of aqueous Cr(VI) using apple wood biochar: a spectroscopic study, J. Hazard. Mater., 384 (2020) 121371, doi: 10.1016/j.jhazmat.2019.121371.
[43] B.Y. Zeng, W.B. Xu, S.B. Khan, Y.J. Wang, J. Zhang, J.K. Yang, X.T. Su, Z. Lin, Preparation of sludge biochar rich in carboxyl/hydroxyl groups by quenching process and its excellent adsorption performance for Cr(VI), Chemosphere, 285 (2021) 131439, doi: 10.1016/j.chemosphere.2021.131439.
[44] X.J. Zhang, L. Zhang, A. Li, *Eucalyptus* sawdust derived biochar generated by combining the hydrothermal carbonization and low concentration KOH modification for hexavalent chromium removal, J. Environ. Manage., 206 (2018) 989–998.